Available online at www.sciencedirect.com
SCIENCE DIRECT®
Journal of Catalysis 224 (2004) 358–369
JOURNAL OF CATALYSIS
www.elsevier.com/locate/jcat

Acetaldehyde reactions over the uranium oxide system

H. Madhavaram and H. Idriss *

Materials Chemistry, Department of Chemistry, The University of Auckland, Private Bag 92016, Auckland, New Zealand

Received 18 November 2003; revised 29 January 2004; accepted 5 March 2004

Available online 17 April 2004

Abstract

To examine the surface reaction of the actinide oxides, the uranium oxide system was considered. The reactions of acetaldehyde are investigated over the surfaces of UO_2, α-U_3O_8, and β-UO_3 by TPD and IR and under flow conditions. The reaction products showed a strong dependency on the O-to-U ratio in the general formula (U_xO_y). Reductive coupling is the dominant pathway on UO_2, triggered by the capacity of the latter to accommodate large amounts of interstitial oxygen (UO_{2+x} with $x \leqslant 0.25$). Aldolization of two molecules of acetaldehyde to crotonaldehyde ($CH_3CH{=}CHCHO$) prevails over α-U_3O_8. Over β-UO_3, the reaction products, at stoichiometric (TPD) as well as under flow conditions, are sensitive to surface coverage. At low coverage a cyclic compound, furan (C_4H_4O), is the dominant product, whereas both furan and crotonaldehyde molecules are formed at high coverage. Moreover, β-UO_3 could be easily transformed to either UO_2 (deep reduction) or α-U_3O_8 (mild reduction) depending on the reaction conditions, and the dynamics between the three phases of the uranium oxides have implications with respect to reaction selectivity. In the absence of oxygen, acetaldehyde gave furan and crotonaldehyde but the selectivity to furan decreased sharply (within a few hours under flow conditions). XRD analyses of the catalyst after the reaction indicated a total transformation to UO_2. The addition of oxygen increased the lifetime of the reaction of acetaldehyde to furan over β-UO_3 but to the detriment of the selectivity. Although addition of oxygen did stop the deep reduction to UO_2, considerable formation of U_3O_8 was observed at the end of the reaction. IR analyses indicated that two modes of adsorption are noted for acetaldehyde depending on the oxide phase. Over UO_3, acetaldehyde is adsorbed exclusively in η^1(O) configuration, while over UO_2, the η^2(C, O) configuration is seen in addition. The latter configuration is reasonably linked to the reductive coupling of two acetaldehyde molecules to $CH_3CH{=}CHCH_3$.

Keywords: UO_2–acetaldehyde; UO_3–acetaldehyde; U_3O_8–acetaldehyde; Acetaldehyde; Temperature-programmed desorption; Acetaldehyde IR; Furan formation from acetaldehyde; Crotonaldehyde formation from acetaldehyde; Acetaldehyde η^1(O) configuration–UO_3; Acetaldehyde η^1(O) configuration–UO_2

1. Introduction

Uranium and uranium oxides have unique electronic structure and properties that have motivated substantial studies by several research groups over the last three decades. Although there is considerable knowledge now of the bulk properties of this oxide system, our understanding of their surface reactions lags that of early transition metal oxides. Among the studies on uranium oxides conducted so far are organometallic investigations [1–4], theoretical calculations [5–7], surface spectroscopy [8,9], and catalytic studies [10–18]. Uranium oxides can be used as catalysts, promoters, or supports for other oxides and metals.

In general, two main catalytic reactions are observed for uranium oxides: (1) oxidation and (2) carbon–carbon bond formation.

1. Uranium–antimony oxide catalysts possess high activity and selectivity in both the supported and unsupported forms for the ammoxidation process [16]. Bismuth–uranium catalysts are active for the oxidative demethylation of toluene [17], as well as for the formation of acrylonitrile and acrolein by ammoxidation and oxidation of propylene, respectively. U_3O_8, both pure and supported on other oxides, is very active for the complete destruction of environmentally undesirable volatile organic compounds [14,15].
2. We have previously shown that U oxides are active for several C–C bond formation reactions: making isobutene from acetone on α-U_3O_8 [18]; making furan from acetylene [19], ethylene [20], acetaldehyde [21],

* Corresponding author. Fax: +64 9 373 7422.
E-mail address: h.idriss@auckland.ac.nz (H. Idriss).

0021-9517/$ – see front matter
doi:10.1016/j.jcat.2004.03.018

or ethanol [22] on β-UO_3; and making ethylene from formaldehyde on UO_2(111) single crystals [23].

In this work we present a study of acetaldehyde reactions over UO_3 and UO_2 by IR and TPD and correlate the data with catalytic studies. We preferred to study acetaldehyde for two reasons. First, it reacts to give a high yield of furan on β-UO_3 [21]; furan is a desired product that enters into a wide variety of chemical compounds [24,25]. Second, acetaldehyde is an *intermediate* molecule that can be easily oxidized or reduced depending on the environment; this is one of the main reasons why acetaldehyde has been studied by several workers over a large number of surfaces including Ru (001) [26], Ag (111) [27], Pt(S)-[6(111) × (100)] [28], Pd (111) [29], Rh (111) [30], $SrTiO_3$(100) [31] and TiO_2 (001) [32] single crystals, and SiO_2 [33,34], TiO_2 [32,35], and CeO_2 [36] powders.

2. Experimental

2.1. Preparation of the oxides

β-UO_3 was prepared from uranium nitrate solution, where $U(OH)_6$ was precipitated using ammonia solution at pH 9. The precipitate was filtered and washed in water. The filtered precipitate was dried at 373 K overnight and calcined at 773 K for 18 h. Polycrystalline α-U_3O_8 was obtained from BDH Chemical and used as is (XRD showed that it comprised exclusively the α phase). UO_2 was prepared by hydrogen reduction of α-U_3O_8 for 10 h at 773 K under hydrogen atmosphere.

2.2. TPD and IR set up

TPD was performed using a fixed-bed reactor interfaced to a high-vacuum chamber equipped with a quadrupole mass spectrometer (base pressure ca. 5×10^{-8} Torr, working pressure during TPD $\approx 5 \times 10^{-7}$ Torr). The reactor pressure during TPD was ca. 10^{-3} Torr at a pumping speed of ca. 10 m^3/h. The mass spectrometer is multiplexed with a PC that is equipped with a program allowing monitoring of 12 masses simultaneously at a cycling rate of ca. 2 s. The ramping rate during TPD was kept fixed at 0.25 $K\,s^{-1}$. Details of the TPD system and of the quantitative data analysis can be found elsewhere [36,37]. Products were analyzed following their m/e as detailed in other works [36,37]. The following masses were used for quantitative analyses: acetaldehyde (m/e 44—parent molecules, m/e 29 (CHO fragment), m/e 43 (CH_3CO)); furan (m/e 68—parent molecule, m/e 39 (C_3H_3)); butadiene (m/e 54—parent molecule, m/e 53 (C_4H_5), m/e 41 (C_3H_5)); butene (m/e 56—parent molecule, m/e 41 and 39); crotonaldehyde (m/e 70—parent molecule, m/e 69 ($CH_3CH{=}CHCO$)). Other products are as described in the text.

FT-IR spectra were recorded with a Bio-Rad–Digilab FTS-60 spectrometer at a resolution of 4 cm^{-1} and 100 scans per spectrum. The experiments were done in situ using a temperature-variable stainless-steel reactor cell equipped with KBr (transmission range 500–4000 cm^{-1}) or CaF_2 (transmission range 1000–4000 cm^{-1}) windows. The cell was operated between 223 and to 773 K. The temperature of the cell was controlled with a calibrated Variac and a type K thermocouple. All experiments were done at a base pressure of ca. 2×10^{-5} Torr.

Pretreatment of the sample always mimicked TPD. This consisted of heating the catalyst sample under O_2 at 523 K for 1 h or under H_2 at 773 K for 10 h. Before introduction of the adsorbate, the sample was evacuated and cooled to 223 K by a flow of liquid nitrogen.

A typical experiment consisted of dosing the reactant onto the pretreated catalyst at 223 K and then pumping the system at that same temperature. Backgrounds of the gas phase and sample prior to dosing were subtracted from all final spectra presented in this work. When several spectra were collected as a function of temperature, the first set was collected after adsorption of the reactant and evacuation at 223 K, then the oxide was heated to the desired temperature and cooled to 223 K (or 300 K) before the spectra were collected.

2.3. Catalytic reactions

Steady-state reactions were carried out in a fixed-bed reactor at different pressures. Three different gas chromatographs (GC) were used to monitor the organic molecules, CO_2 and CO. The reactor was placed in a programmable oven connected to a GC, equipped with flame ionization detector (FID), via a six-way valve. To separate the products, a Chromosorb 102 column was used. The GC was coupled to a PC running PEAKSIMPLE III software for data acquisition. A Hewlett Packard 6890 gas chromatograph coupled with a Hewlett Packard 5973 mass selective detector (GC/MS) was also used. The GC employed a Gas Pro GSC capillary column of 30 m × 0.32 mm i.d. with helium as carrier gas. The capillary column was temperature programmed with an initial temperature of 473 K for 2 min, then ramped at 20 K/min to 513 K. The mass selective detector was set to record mass spectra in the range 10 to 500 amu at predetermined rate of three scans per second. A split ratio of 30:1 was used, i.e., 1/30th of the sample volume was injected into the GC/MS. A 5-ml Hamilton gasproof lockable syringe was used to inject the gas samples into the GC/MS. To monitor CO and CO_2, a GC operating isothermally at 300 K and equipped with a thermal conductivity detector (TCD) and a Chromosorb 102 column was used.

3. Results

3.1. Temperature-programmed desorption studies over UO_2, U_3O_8, UO_3, and Al_2O_3

3.1.1. TPD after acetaldehyde adsorption over β-UO_3

Figs. 1a and b and Table 1 present desorption profiles during acetaldehyde TPD on β-UO_3 at two different representative initial exposures (270 and 6 Torr min). At low surface exposure, mainly acetaldehyde (m/e 29) and furan (m/e 68 and 39) are observed, in addition to CO_2. At high coverage, crotonaldehyde (m/e 70) is seen in addition (33%). Other C4 products are also seen: butadiene (m/e 54) and butenes (m/e 56) (about 20%). Traces of ethanol (m/e 31, 46, 45), crotyl alcohol (m/e 72), and acetone (m/e 43, 58, 15), with a combined carbon selectivity of less than 1%, also desorbed. CO_2 (m/e 44) desorbed at 650 K. The large amount of CO_2 is due mainly to carbonate decomposition of the *as-prepared* β-UO_3, because it is also observed on the blank oxide (see the inset to Fig. 1a; IR also shows the presence of these carbonates that decompose at high temperature, see Section 3.3). No evidence was found for the aldol desorption, $CH_3CH(OH)CH_2CHO$ (m/e 88), the aldolization product before dehydration to crotonaldehyde. No detectable signal was observed for m/e 132 corresponding to the cyclic trimer, trimethyl trioxane, which has been reported on some metal surfaces [38]. Moreover, the signal for m/e 60 was absent throughout the temperature range examined; thus, direct oxidation of acetaldehyde to acetic acid is ruled out.

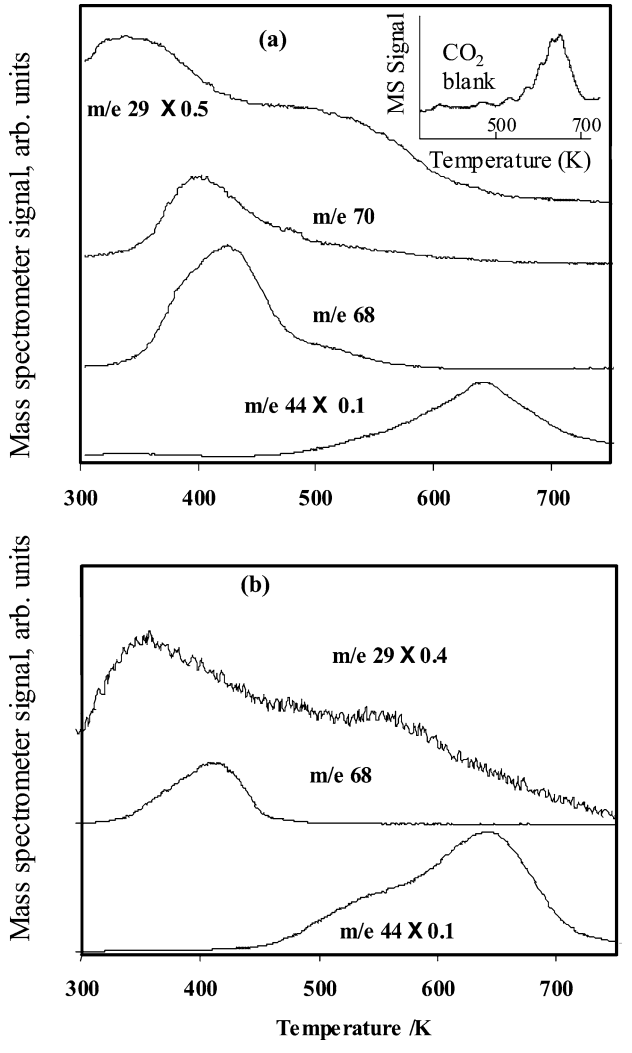

Fig. 1. TPD of acetaldehyde at two different exposures over β-UO_3: (a) high exposure (270 Torr min), (b) low exposure (6 Torr min). Most of the acetaldehyde is converted into furan (m/e 68) at low exposure.

3.1.2. TPD after acetaldehyde adsorption on α-U_3O_8

Carbon selectivity of products formed during TPD after acetaldehyde adsorption at room temperature on α-U_3O_8 is summarized in Table 1, while Fig. 2 presents the raw TPD data. The main difference with the β-UO_3 data is the negligible amounts of furan and the large amounts of crotonaldehyde. This observation was not dependent on surface coverage. Most of the C4 hydrocarbons have disappeared and the presence of a mass m/e 86, with considerable intensity, is detected. Because no other masses above m/e 86 were observed, we considered m/e 86 as the parent fragment

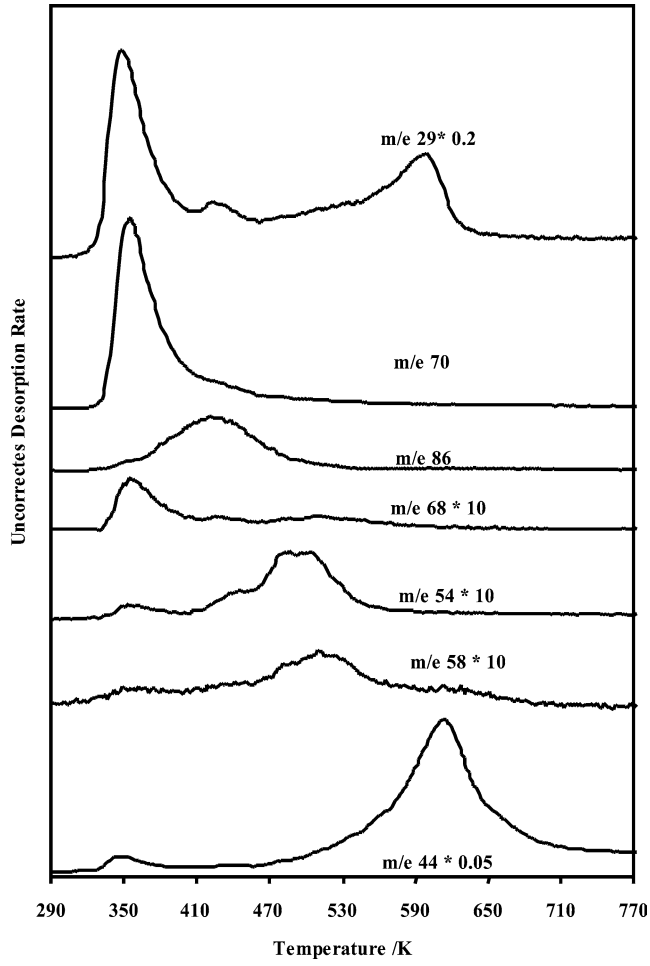

Fig. 2. TPD of acetaldehyde over α-U_3O_8.

of a product formed from acetaldehyde on α-U_3O_8 during TPD. With respect to the C4 oxygen-containing molecules m/e 86 might be one of the following products: crotonic acid (CH_3–CH=CH–COOH), γ-butyrolactone ($C_4H_6O_2$), or 2,3-butanedione ($CH_3C(O)C(O)CH_3$). Analyses of the fragmentation pattern in the same temperature domain as that of m/e 86 (430 K) rejects γ-butyrolactone ($C_4H_6O_2$) due to the absence of m/e = 56 (main fragment of γ-butyrolactone). Crotonic acid gives m/e 86 as the parent ion fragment; other fragments with high intensity are m/e 41, 39, and 68. The absence of m/e 68 at the same desorption temperature as m/e 86 rules it out. 2,3-Butanedione has m/e 86 and m/e 43 as major fragments in the ratio $\approx 1/5$. It is made from the monoketone by oxidation over zeolite catalysts [39]. The presence of both desorption products at 430 K leads to the assignment as the diketone.

3.1.3. TPD after acetaldehyde adsorption on UO_2

TPD after acetaldehyde adsorption on UO_2 at room temperature is illustrated in Fig. 3, and the carbon selectivity of products is summarized in Table 1. While furan was the main product on β-UO_3 and crotonaldehyde was the main product on U_3O_8, ethanol and the C4 hydrocarbons (butadiene and butene) were the main products on UO_2. Acetaldehyde (m/e 29, 15, 44) desorbed as one main peak, followed by a weak desorption above 450 K. Ethanol (made by reduction) desorbed at 580 K (36%) while the C4 hydrocarbons (reductive coupling)—butadiene (m/e 54, 39, 53) and butene (m/e 56, 41, 39)—desorbed at 540–550 K with a combined carbon selectivity of 33%. Clearly, UO_2 favors the reduction processes. Some crotonaldehyde also desorbed at 350 K, while CO_2 (m/e 44) desorbed with a complex set reaching a maximum at 650 K. All potential higher-molecular-weight products described in β-UO_3 and α-U_3O_8-acetaldehyde TPD were looked for but not found.

3.1.4. TPD after acetaldehyde adsorption on γ-Al_2O_3

γ-Al_2O_3 is a common support for many catalysts and is widely used. A comparison with the U–O system would help in differentiating the TPD reaction products. *The main observation is that formation of furan and the C4 hydrocarbons was negligible*. The carbon selectivity of products and raw data are shown in Fig. 4 and Table 1. Acetaldehyde (m/e 29, 15, 44) desorbed as a peak with a maximum at 380 K. Crotonaldehyde was the major product desorbing at 390 K (69%). Ethanol desorbed at 420 K with a yield of 15%. Acetone desorbed at a higher peak temperature, 730 K, with a similar yield.

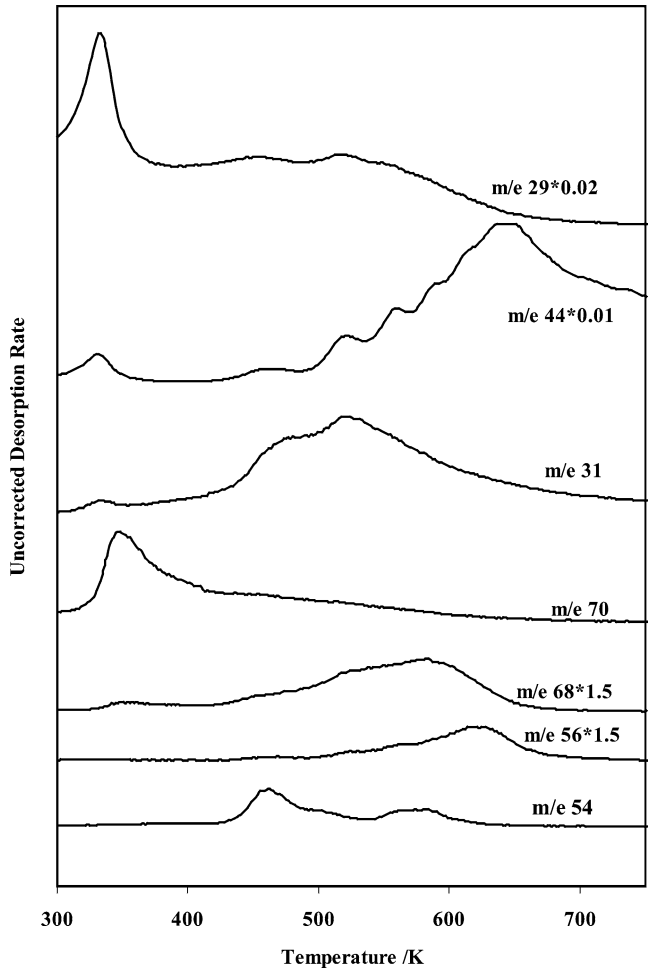

Fig. 3. TPD of acetaldehyde over UO_2.

From the above TPD results we learn the following. Furan is formed mainly over β-UO_3 at low acetaldehyde exposure. Ethanol and C4 hydrocarbons are formed mainly on UO_2. The yield of crotonaldehyde is highest over α-U_3O_8 and this reaction is similar to that on γ-Al_2O_3.

3.2. Catalytic reactions

Steady-state reactions were performed with acetaldehyde over β-UO_3 to investigate the role of gas-phase oxygen and to make furan production from acetaldehyde a catalytic reac-

Table 1
Carbon selectivity (%) of the different reaction products, during acetaldehyde TPD over β-UO_3, α-U_3O_8, UO_2, and Al_2O_3 surfaces

	β-UO_3	α-U_3O_8	UO_2	γ-Al_2O_3
Furan (m/e 68)	48 Coupling	1	7	1
Crotonaldehyde (m/e 70)	33 Aldolization	68 Aldolization	15	69 Aldolization
2,3-Butanedione (m/e 86)	–	25 Oxidation	–	–
Acetone (m/e 58)	–	3	8 Coupling	15 Coupling
C4 hydrocarbons	19	2	37 Reductive coupling	–
Ethanol (m/e 31)	–		33 Reduction	15 Reduction

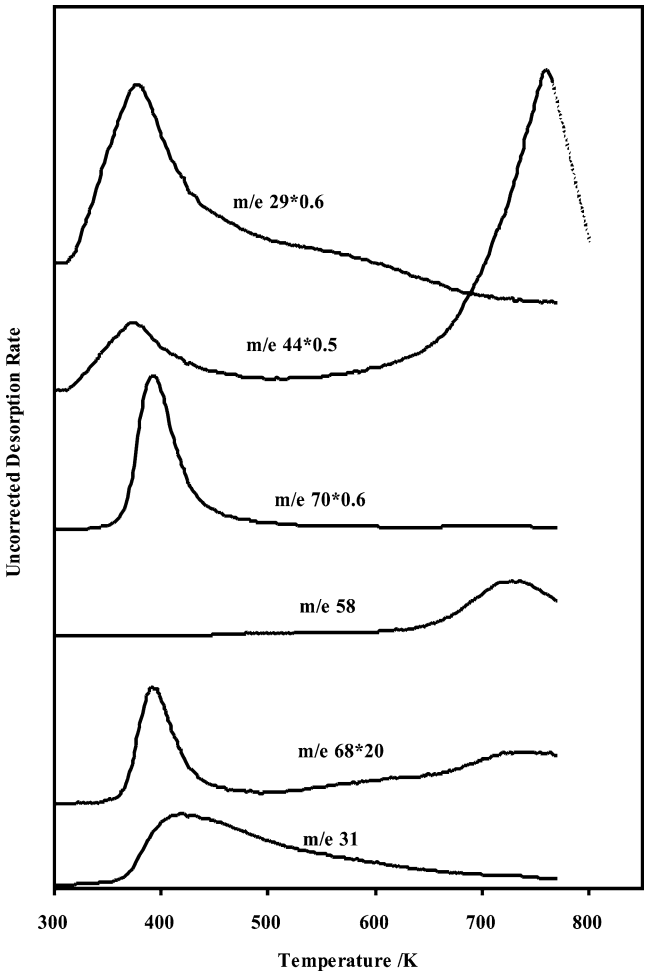

Fig. 4. TPD of acetaldehyde over Al_2O_3.

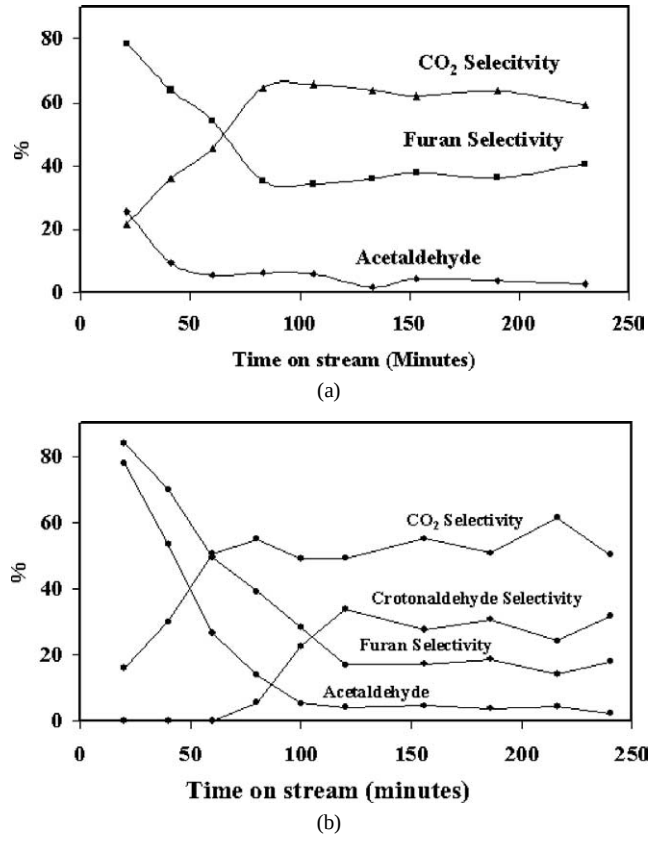

Fig. 5. Furan and CO_2 selectivity as a function of time-on-stream over β-UO_3. $[CH_3CHO] = 1.2 \times 10^{-7}$ mol ml^{-1}, $F/W = 25$ ml min^{-1} g_{cat}^{-1}. (a) $T = 523$ K, (b) $T = 573$ K.

tion. At 473 K furan was the only detectable product and the catalyst was deactivated after about an hour. Fig. 5a presents the steady-state reactions at 523 K with an acetaldehyde concentration of 1.2×10^{-7} mol/ml. The longer the reaction was left, the more CO_2 was produced. No other organic products were observed. When the reaction temperature was increased to 573 K, crotonaldehyde was also observed, as shown in Fig. 5b. XRD (Fig. 6) of the catalyst collected at the end of the 573 K run revealed large amounts of UO_2.

Because catalyst deactivation occurred very rapidly, along with acetaldehyde, oxygen (acetaldehyde:O_2 = 4:1) was co-fed. The introduction of oxygen resulted in the reappearance of furan and also retarded deactivation of the catalyst. However, formation of other organic compounds increased, mainly formaldehyde and acrolein (CH_2=CHCHO) along with crotonaldehyde as shown in Fig. 7. The presence of oxygen had a mild effect on acetaldehyde conversion (as shown in Fig. 7b). XRD (Fig. 8) of this catalyst after the reaction showed that the presence of oxygen inhibited the transformation to UO_2, but considerable transformation to α-U_3O_8 occurred. It is thus reasonable to suggest that the decrease in reaction selectivity is due to the bulk transformation, obviously carrying with it a different surface environment.

3.3. Infra red spectroscopy study

As TPD and catalytic reactions have shown that acetaldehyde gives furan and crotonaldehyde on β-UO_3 while ethanol and C4 hydrocarbons are formed over UO_2, we conducted in situ IR to probe into the surface species following the adsorption of acetaldehyde over both oxides.

3.3.1. IR spectra of β -UO_3

3.3.1.1. After adsorption of acetaldehyde at 223 K Fig. 9 and Table 2 present IR bands obtained after exposing β-UO_3 to acetaldehyde at saturation (1.6×10^6 L) at 223 K. IR spectra were then taken at different temperatures. Spectrum **a** shows the following IR bands: 2984, 2907, 1706 1576, 1448, 1412, 1380, 1350, 1174, 1145, 1125, and 1100 cm^{-1}. The bands at 2984 ($\nu_{as}(CH_3)$), 2907 ($\nu_s(CH_3)$), 1706 (ν(CO)), 1412 ($\delta_{as}(CH_3)$), 1350 ($\delta_s(CH_3)$), 1380 (δ(CH)), 1125 ($\gamma(CH_3)$, ν(C–C)) cm^{-1} are assigned to adsorbed acetaldehyde [40]. The bands at 1576 (ν_{as}(OCO)) and 1448 (ν_s(OCO)) cm^{-1} are attributed to bidentate acetate species ($\nu_{as}(OCO) - \nu_s(OCO) = \Delta = 128$ cm^{-1}). The formation of acetate species from acetaldehyde molecules was

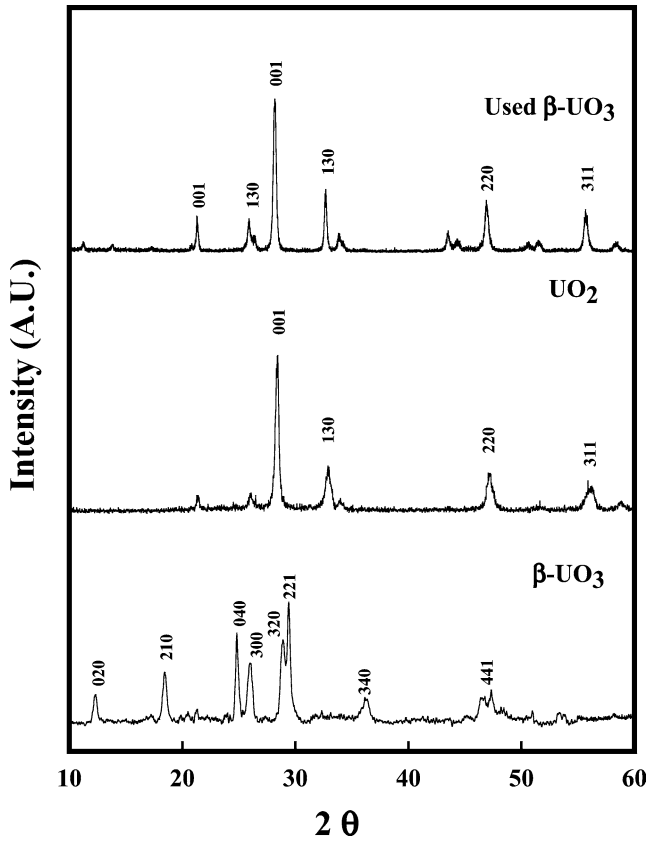

Fig. 6. XRD of fresh β-UO_3 and of β-UO_3 after acetaldehyde reaction in the absence of oxygen (used catalyst); UO_2 is added as a reference.

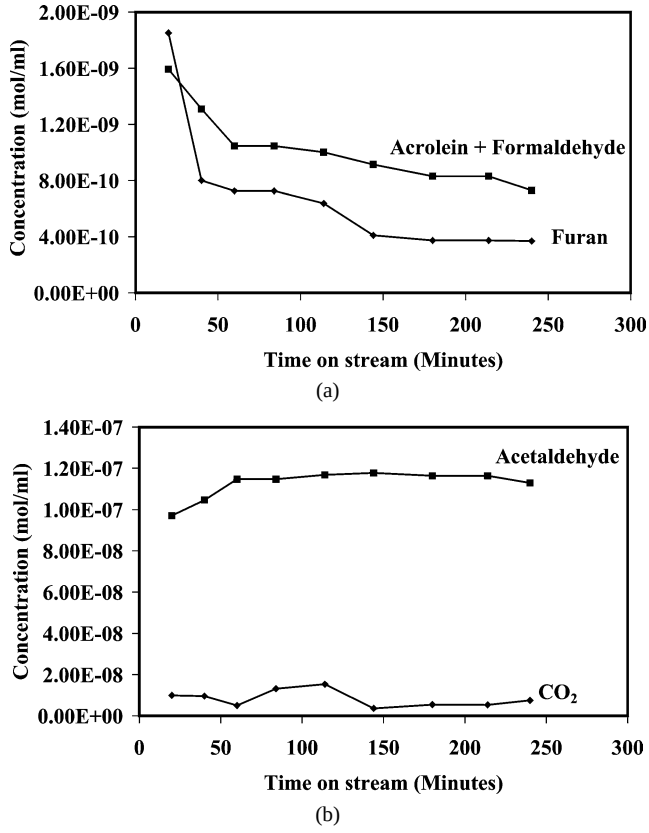

Fig. 7. Effect of oxygen on (a) furan production from acetaldehyde and (b) acetaldehyde conversion.

previously observed on several oxide species including TiO_2 [32], ZnO [41], and CeO_2 [36] (Table 3). No clear bands attributed to ethoxide species could be observed. The absence of ethoxide species explains the absence of ethanol during TPD; the reduction reaction is not favored on β-UO_3.

Spectra **b** and **c** were obtained after heating the surface of spectrum **a** to 316 and 380 K, respectively. The bands at 2987, 2907, 1706, 1350, 1145, 1100, and 1125 cm^{-1} disappeared (adsorbed acetaldehyde). Along with the disappearance of these bands, new bands attributed to adsorbed crotonaldehyde species appeared at 1657 (ν(C=C)), 1636 (δ(CH)), and 1400 (δ(CH)) cm^{-1} [36,42]. The bands at 1520 (ν_{as}(COO)), 1439 (ν_s(COO)), and 1320 (ν(CO)) cm^{-1} are attributed to bidentate carbonate species [36,42] (Table 4). On heating to 420 K the peaks corresponding to adsorbed crotonaldehyde and acetate species decreased in intensity, while those due to bidentate carbonate species increased. Carbonates remained the dominant species on the surface up to 608 K. On further heating to 754 K carbonates were totally removed. To observe bands associated with adsorbed furan molecules on the surface, furan was dosed on the surface in a separate run.

3.3.1.2. After adsorption of furan Fig. 10 shows two IR spectra collected on adsorption of furan (at different dosing pressures) over β-UO_3 surface. Although few studies have dealt with furan spectroscopy over metals and none on an oxide surface to date, some information can be obtained from two main works conducted by Sexton [43] and Ormerod et al. [44] on Cu(100) and Pd(111) single crystals, respectively, as well as from the IR of furan in the gas-phase (Table 5). Furan is characterized by several IR bands belonging to both the ring and CH modes. The band at 1055 cm^{-1} is assigned to ν(C–O) and ν(C–C). The weak band at 1170 is due to ρ(CH) and ν(C=C), actually this band is very strong in the gas-phase. The small band at 1277 cm^{-1} is that of ρ(CH) while the band at 1373 cm^{-1} is that of ρ(CH) and ν(C–C). There is a large band at 1570–1630 cm^{-1}. This band most likely contains contributions of ν(C=C) and ρ(CH), the presence of some bending mode of adsorbed wa-

Table 2
IR vibrational frequencies (cm^{-1}) and mode assignments of acetaldehyde adsorption on β-UO_3 and various metal oxides from the literature

Assignment	Gas [40]	Anatase, TiO_2 [52]	SiO_2 [53]	β-UO_3, this work	UO_2, this work
$\nu_{as}(CH_3)$	3003	2969	2988	2984	2987
$\nu_s(CH_3)$	2918	2914	2914	2907	2934
ν(CO)	1722	1718	1724	1706	1705
$\delta_{as}(CH_3)$	1422	–	1448	1412	1450
δ(CH)	1389	–	1388	1380	1380
$\delta_s(CH_3)$	1352	1355	1356	1351	1340
$\gamma(CH_3)$, ν(C–C)	1120	–		1125	1123

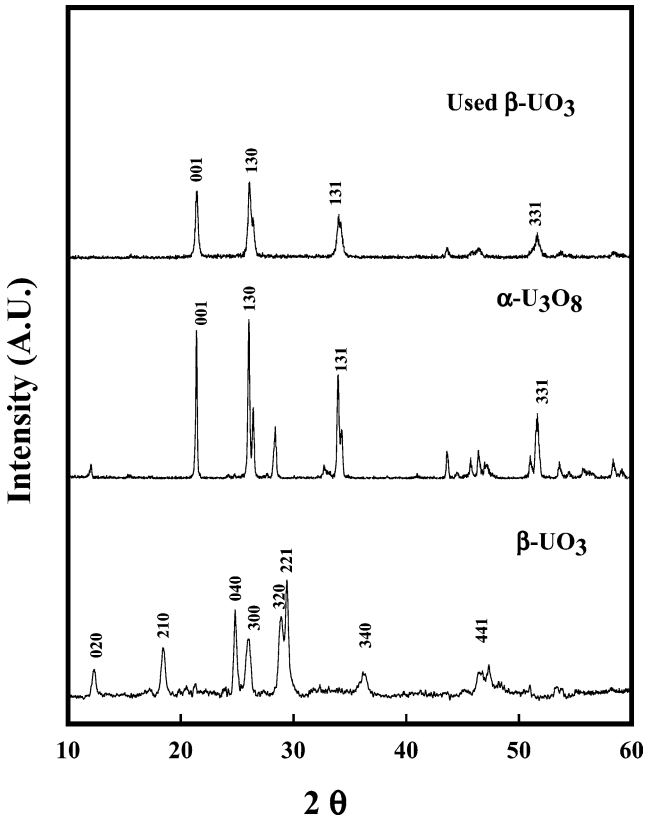

Fig. 8. XRD of fresh β-UO_3 and of β-UO_3 after acetaldehyde reaction in the presence of oxygen (used catalyst); α-U_3O_8 is added as a reference.

ter is also possible at ca. 1600 cm^{-1}. From these data one can make the following claims: (1) Furan is weakly adsorbed on β-UO_3. This is confirmed by TPD conducted after furan adsorption on β-UO_3 (Fig. 11) where the main desorption peak was seen at 350 K (lower than that seen during furan desorption from acetaldehyde, Fig. 1). (2) Part of the furan is most likely lying on the surface (near absence of the band at 1170 cm^{-1}, yet very strong in the gas phase). In other words the C–O stretching of a molecule not parallel to the surface should have been more pronounced. With the help of these spectra one would in principle identify furan in acetaldehyde IR studies. Yet, because the most intense band from furan is at 1570–1630 cm^{-1}, as seen in Fig. 10, and since acetate species give bands at about 1550–1570 cm^{-1}, it was not possible to claim the presence or absence of adsorbed furan species from acetaldehyde IR.

3.3.2. IR spectra of UO_2

3.3.2.1. After adsorption of acetaldehyde at 223 K Fig. 12, spectrum **a**, shows IR bands obtained after exposing UO_2 to acetaldehyde at 223 K. A different set of surface adsorbates are observed when compared with those obtained on adsorption of acetaldehyde on β-UO_3 (Fig. 9). The following is a step-by-step analysis of the different bands and their attributions.

The CH region is far more resolved than in the case of acetaldehyde–β-UO_3. The two bands at 2987 and 2934 cm^{-1} are most likely from $\delta_{as}CH_3$ and δ_sCH_3 of acetaldehyde, respectively. The wide band on the lower wavenumber side of 2934 cm^{-1} might originate from ν(CH) (the gas-phase ν(CH) is close to 2820 cm^{-1}). Below 1750 cm^{-1} several bands are observed. Some can be attributed to adsorbed acetaldehyde. However, unlike in the case of UO_3, it appears that two modes of acetaldehyde are present: a monodentate mode (η^1) and a bidentate mode (η^2). In an ideal bidentate configuration the IR band at ca. 1700 cm^{-1}, attributed to C=O, would be very weak, as it is parallel to the surface. In effect, due to rehybridization it has been shown that for the η^2 mode of acetaldehyde, the C=O bond is shifted to ca. 1400 cm^{-1} [45]. One may then assign all the C=O stretching at the 1705 cm^{-1} position as due to η^1 adsorbed acetaldehyde. On the other hand, assignment of a band to η^2(C,O) in our case is not clear. In spectrum **a**, the 1400 cm^{-1} region contains multiple peaks and one cannot conclude for sure that the C=O of η^2 is indeed observed. However, other bands might help. In fact, another major difference between both modes of acetaldehyde is related to the ν(C–C) mode at 1100–1200 cm^{-1}. Comparison of Fig. 12 with Fig. 9 indicates that the 1123 cm^{-1} band (observed at 1125 cm^{-1} in Fig. 9), is far larger in the UO_2 case. The ν(C–C) vibration has also been seen to be more pronounced for η^2(C,O) than for η^1(O) acetaldehyde in other works [26]. Then the large intensity of the 1705 cm^{-1} peak associated with the small intensity of the 1125 cm^{-1} peak in Fig. 9 suggests that acetaldehyde is mainly in a η^1 mode. Conversely, the small intensity of 1705 cm^{-1}, associated with the large intensity of 1123 cm^{-1} in Fig. 12, strongly suggests the presence of considerable amounts of the η^2 mode of adsorbed acetaldehyde. The band at 1548 cm^{-1} is attributed to the ν_{as}(COO) surface acetate formed by oxidation of some acetaldehyde. The band at 1450 cm^{-1} is due to ν_s(COO) with some contribution from the asymmetric CH_3 deformation mode and probably some contribution from the ν(C=O) mode of acetaldehyde. The band at 1340 cm^{-1} is due to δ_s of CH_3 of both acetaldehyde and acetate species. The band at 1380 cm^{-1} might originate from the CH bending mode of acetaldehyde. The rocking mode of acetaldehyde is observed at 912 cm^{-1} and this is consistent with both gas-phase and with HREELS data of η^2 adsorbed acetaldehyde over a variety of metals (Table 6). The band at 1068 cm^{-1} is attributed to an ethoxide-type species.

On heating to 280 K several features were observed. The band corresponding to adsorbed acetaldehyde at 1123 cm^{-1} decreased. An increase in the acetate species at 1548 and 1450 cm^{-1} was also observed. Heating to 374 K resulted in complete disappearance of the bands corresponding to ethoxide species at 1068 cm^{-1}. A further increase in acetate bands also occurred. In addition, prominent bands appeared at 1657, 1637, 1612, 1114, 1028, and 958 cm^{-1}. On further heating to 493 and 653 K we see an increase in the bidentate acetate bands along with a shift to ν_{as}(OCO) 1536, ν_s(OCO) 1435, and $\delta_s(CH_3)$ 1343 cm^{-1}. By 750 K, bands at

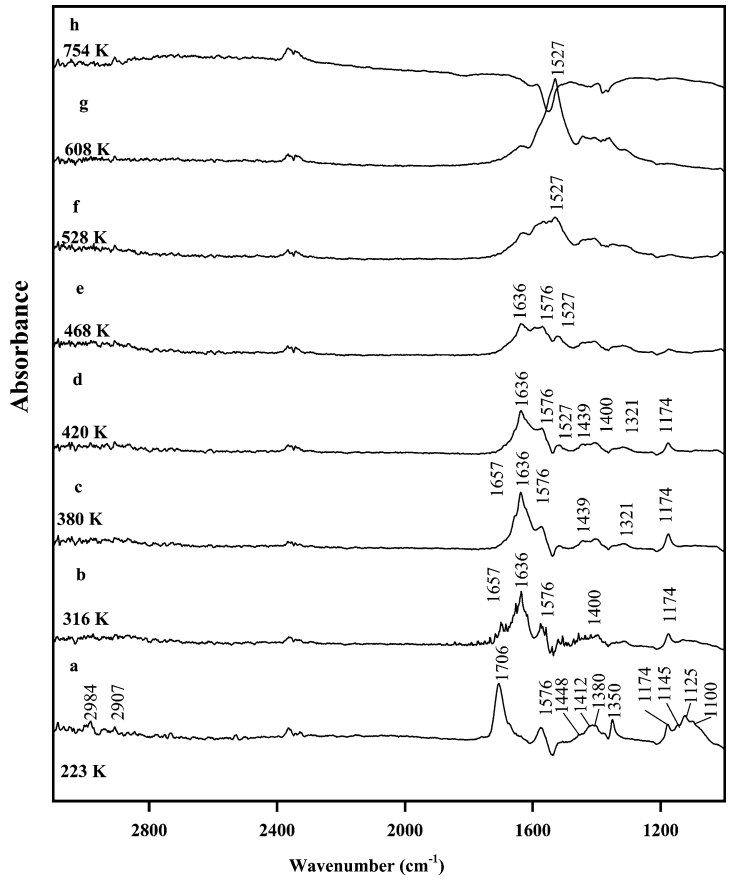

Fig. 9. FTIR of acetaldehyde over β-UO_3.

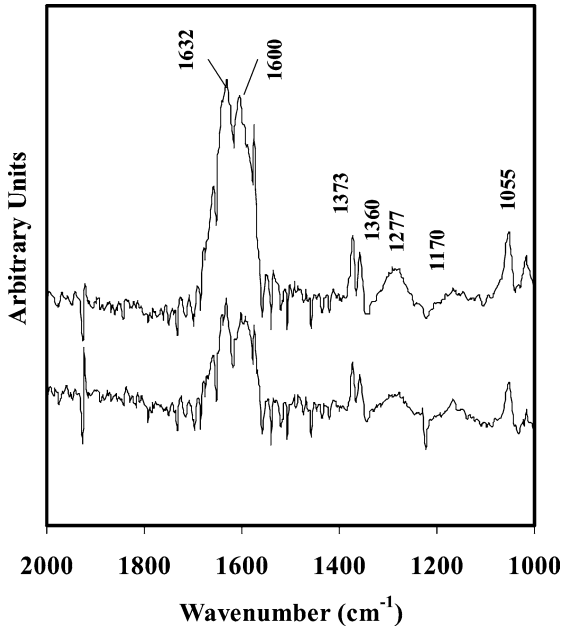

Fig. 10. IR of furan adsorbed over β-UO_3.

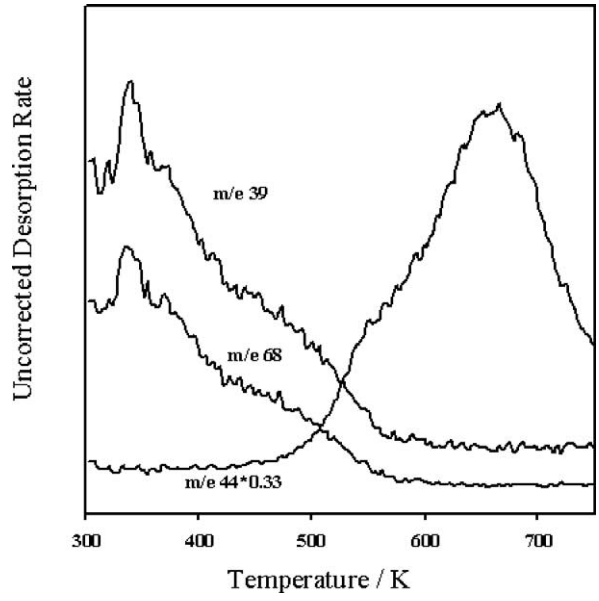

Fig. 11. TPD of furan over β-UO_3.

1556, 1505, and 1396 cm^{-1} attributed to bidentate carbonates dominate the surface.

TPD indicated that, besides desorption of acetaldehyde and ethanol, three other products are observed; all are due to C–C bond formation. These products are crotonaldehyde, furan, and butadiene. The bands at 1662 (ν(C=C)), 1600, 1404, 1160 (ν(C–C), $\rho(CH_3)$), 1108 (ν(C–C)), and 968 ($\rho(CH_3)$) cm^{-1} are attributed to crotonaldehyde.

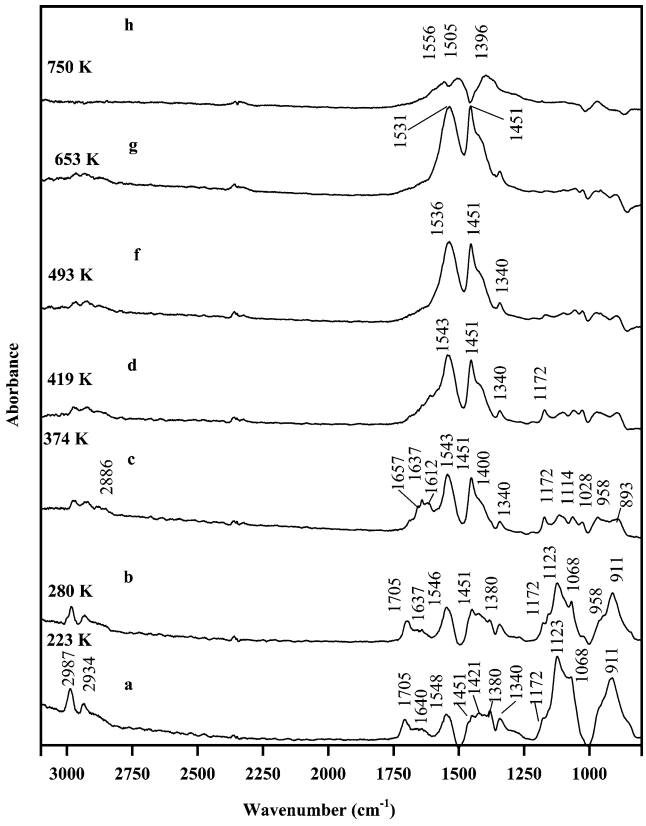

Fig. 12. FTIR of acetaldehyde over UO_2.

Table 3
IR vibrational frequencies (cm^{-1}) and mode assignments for adsorbed acetate species from the adsorption of acetic acid on various metal oxides

Assignment	α-Fe_2O_3 [54]	ZnO [55]	TiO_2 [56]	CeO_2 [37]	UO_2, this work
$\nu_{as}(CH_3)$	–	–	3018	2970	
$\nu_s(CH_3)$	–	2940	2939	2933	
$\nu_{as}(OCO)$	1540	1554	1587	1580	1536
$\delta_{as}(CH_3)$	–	1460	1459, 1672	1437	–
$\nu_s(OCO)$	1427	1427	–	1426	1435
$\delta_s(CH_3)$	–	1311	1421	1304	1343
$\rho(CH_3)$	–	–	1334	1051, 1026, 1019	

Table 4
η^2-Acetaldehyde HREELS assignments; frequency (cm^{-1})

Assignment	Gas phase	Multilayer	Ru [26]	Rh [30]	Pd [29]
$\nu(CH_3)$	2964, 2918	3000	2970	2980	2990
ν(C=O)	1722	1745	1395	1460	1390
$\delta(CH_3)$	1431, 1389	1450	1340	1380	1390
ν(C–C)	1118	1135	1095	1135	1080
$\rho(CH_3)$	882	920	915	950	930
δ(C–C–O)	522	545	605	610	600

The presence of butadiene during TPD (Fig. 3), suggesting a reductive coupling reaction, indicates that a reaction intermediate in the form of a pinacolate might be present (see reaction mechanism in Scheme 1). We have recently observed formation of ethylene from formaldehyde over UO_2 powder and UO_2(111) single crystal [23] and other workers have also observed the same on Mo(110) single crystal [46,47]. This is analogous to obtaining butene from acetaldehyde via a 2,3-butanediolate intermediate as shown in Scheme 1.

We have thus studied the adsorption of 2,3-butanediol on the surface of UO_2.

Table 5
IR and HREELS frequencies (cm^{-1}) and mode assignments for gas-phase and adsorbed furan

Assignment	Gas [57]	Cu(111) [43]
ν(CH)	3167	–
ν(CH)	3161	3150
ν(CH)	3140	–
ν(CH)	3129	–
ν(C=C) + ρ(CH)	1556	–
ν(C=C) + ρ(C–C)	1491	1510
ρ(CH) + ν(C–C)	1384	1400
ρ(CH)	1267	–
ν(C–O) + ρ(CH)	1180	1190
ρ(CH) + ν(C=C)	1140	–
ν(C–O) + ν(C–C)	1066	1070
ρ(CH) + ν(C–O) + ν(C=C)	1040	–
ρ(CH) + ν(C–O) + ν(C=C)	995	1010
Ring deformation	873	–
Ring deformation	871	880
ω(CH)	863	–
ω(CH)	838	–
ω(CH)	745	760
ω(CH)	728	–
Ring torsion	613	–
Ring torsion	603	600

Table 6
IR vibrational frequencies (cm^{-1}) and mode assignments from the adsorption of crotonaldehyde on various metal oxides

Assignment	Gas phase [54]	TiO_2 anatase [52]	SiO_2 [53]	Pd/CeO_2 [37]
ν(C=C–H)	3058	3038	3042	–
$\nu_{as}(CH_3)$	2963	2954	2951	–
$\nu_s(CH_3)$	2738	2920	2924	–
ν(CH)	2728	2745	2744	–
ν(C=O)	1728	1686	1688	1651
ν(C=C)	1649	1636	1642	1634
$\delta(CH_3)$	1391	1394	–	1395
$\rho(CH_2)$, ν(C–C)	1147	1165	–	1160

3.3.2.2. After adsorption of 2,3-butanediol 2,3-Butanediol was adsorbed on the surface of UO_2 at 223 K (Fig. 13). Adsorption of 9 Torr at 3 min corresponded to surface saturation. Several bands are observed (in cm^{-1}): 2967 ($\nu_{as}(CH_3)$), 2927 (ν(CH)), 2866 ($\nu_s(CH_3)$), 1746 (ν(C=O)), 1630 (the gas-phase ν(C=O) of 2,3-butanedione is at $\approx$ 1750 cm^{-1}), 1568 (ν_{as}(COO)), (most likely from a carboxylate formed by further reaction with the surface), 1462 (ν_s(COO) of a carboxylate), 1445 ($\delta_{as}(CH_3)$), 1381 ($\delta_s(CH_3)$), 1349 (δ(CH)) of the diol. The only detailed work of a diolate adsorbed on a surface is that of ethylene glycol

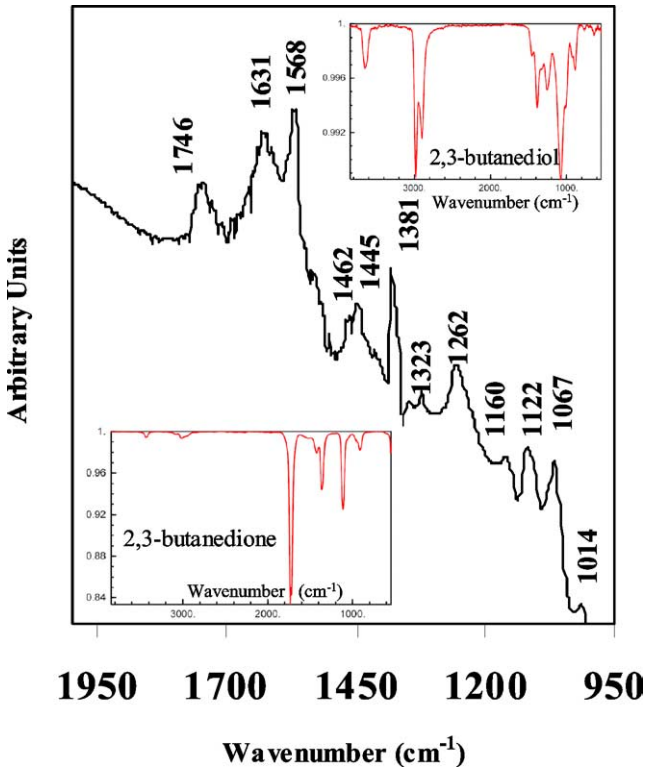

Fig. 13. IR of 2,3-butanediol over UO_2. The gas-phase IR of 2,3-butanediol and 2,3-butanedione (from http://webbook.nist.gov/chemistry) are shown for comparison.

(HO–CH_2CH_2–OH) on Mo(110) single crystal by HREELS [46,47] and it is with the help of this work and that of ethanol on CeO_2 [37] that the other bands are analyzed. A band at ca. 1262 cm^{-1} has been observed for molecularly adsorbed ethanol. The shape and position of the band are very similar to those observed at 1260–1264 cm^{-1} from ethanol on M/CeO_2 [42]. By analogy, the band at 1262 cm^{-1} (Fig. 13) can be attributed either to an OH bending mode (δ(OH)) of a monodentate adsorbed species (HO–CH_2CH_2–O(a), where (a) denotes adsorbed) or to that of surface OH. In Ref. [47] a band at 1008 cm^{-1} is observed at low coverage and attributed to ν(O–C) of pinacolates ((a)O–CH_2–CH_2–O(a)). When surface saturation was approached, a strong band was observed at a higher frequency (1080 cm^{-1}) in addition. They attributed this new band to the ν(O–C) of a monodentate species. From Figs. 12 and 13 and Refs. [42,46,47] one can conclude the following. The IR band at 1068 cm^{-1} formed from acetaldehyde at 220 K and disappearing by 380 K is due to ν(O–C) of either ethoxide or pinacolate species.

4. Discussion

Results from this work can be summarized as follows.

1. On UO_3, acetaldehyde gives furan at low exposure and furan and crotonaldehyde at surface saturation.
2. On U_3O_8, crotonaldehyde is the main product observed.
3. On UO_2, reduction to ethanol competes with the reductive coupling to C4 hydrocarbons.
4. Flow reactions of UO_3 show that furan production decreases sharply with time and this is concomitant with bulk transformation of UO_3 to UO_2. In presence of oxygen, this transformation is delayed and partial reduction to U_3O_8 is observed.

The following scheme shows the different reactivity of the uranium oxide system vis-à-vis acetaldehyde.

$$2CH_3CHO + \mathbf{UO_3} \rightarrow C_4H_4O + 2H_2O + \mathbf{UO_2}, \quad \Delta H_f^\circ = -47\ \mathrm{kJ\,mol^{-1}}, \tag{1}$$

$$2CH_3CHO + \mathbf{3UO_2} \rightarrow CH_3CH{=}CHCH_3 + \mathbf{U_3O_8}, \quad \Delta H_f^\circ = +1\ \mathrm{kJ\,mol^{-1}}, \tag{2}$$

$$2CH_3CHO \xrightarrow{\mathbf{U_3O_8}} CH_3CH{=}CHCHO + H_2O, \quad \Delta H_f^\circ = -10\ \mathrm{kJ\,mol^{-1}}. \tag{3}$$

In the presence of O_2 Eq. (1) becomes

$$2CH_3CHO + \mathbf{3UO_3} + O_2 \rightarrow C_4H_4O + 2H_2O + \mathbf{U_3O_8}, \quad \Delta H_f^0 = -90\ \mathrm{kJ\,mol^{-1}}. \tag{4}$$

U_3O_8 in Eq. (2) is not necessarily formed; instead UO_{2+x} can be made during TPD. Once U_3O_8 is formed in (4) it triggers the catalytic formation of formaldehyde and acrolein, presumably via the decomposition of furan.

The discussion focuses on three points. (1) The thermodynamic equilibrium of the uranium oxide and its implication in surface chemistry. (2) Why UO_3 orients to furan while U_3O_8 orients to crotonaldehyde. (3) What are the plausible reaction mechanisms for the formation of furan and C4 hydrocarbons.

The dynamics in U $\leftrightarrow$ UO_2 $\leftrightarrow$ U_3O_8 $\leftrightarrow$ UO_3 have been studied extensively, mostly by nuclear chemists, and several detailed reviews are available [48]. Although UO_3 (γ-form) is thermodynamically stable and should be obtained from U or UO_2 at 973 K and above, in practice air oxidation yields U_3O_8, indicating its more complex behavior depending on time and O_2 partial pressure. O_2 diffusion into the bulk of UO_2 is relatively fast. The activation energy (ΔH) for the diffusion of O atoms into the bulk is estimated to be equal to $\approx$ 100 kJ/mol. The diffusion coefficient for O into UO_{2+x} at 1000 K was found to be equal to 1.5×10^7 $nm^2\,s^{-1}$ [49]; it is relatively insensitive to x. From these two values and the knowledge that $D = D_0 \exp(-E_a/RT)$, we computed O diffusion at 600 K (where most of the reaction occurred) in UO_2 as equal to 7×10^3 $nm^2\,s^{-1}$, far higher on the atomic scale than TPD ramping (0.25 $K\,s^{-1}$). This number explains the transformation of UO_2 to U_3O_8 (via UO_{2+x}, U_3O_7, and U_4O_9) during acetaldehyde TPD in the process of making hydrocarbons. UO_3 can be easily reduced to U_3O_8 by hydrogen [18]. Both oxides end up being transformed to UO_2 at 1 atm of H_2 at 700 K. ΔH_f° for U_3O_8 to UO_2 reduction

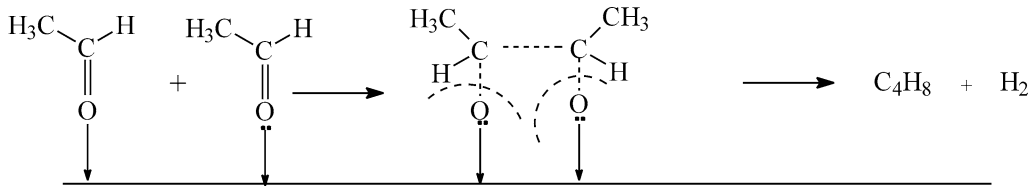

Scheme 1.

with H_2 is equal to 120 kJ mol^{-1} [50]. This small activation energy explains the following observations: (1) By the end of the TPD run, UO_3 has been transformed to U_3O_8 and some UO_2 (XRD). (2) Catalytic reactions under acetaldehyde flow (in the absence of O_2) at 573 K show that UO_3 is transformed to UO_2 after about 4 h (XRD). (3) IR shows that carbonates of UO_3 are decomposed by 700 K.

Other workers have shown that furan can be made from crotonaldehyde on Cu catalysts [51]. The presence of IR bands attributed to crotonaldehyde and the (most likely) absence of bands attributed to furan indicate that acetaldehyde initially undergoes a condensation to an adsorbed crotonaldehyde. β-UO_3 is made of U^{6+} cations while U_3O_8 is made of U^{6+} and U^{4+} cations in a 2:1 ratio. Their structures are different. β-UO_3 has a complex monoclinic structure with the unit cell composed of five U cations; three of them are 6-fold coordinated and the other two are 7-fold coordinated. U_3O_8 has an orthorhombic structure, with all U cations in pentagonal bipyramid structure (7-fold coordinated). We have previously related the presence of the 6-fold U^{6+} cations (found only in UO_3; U can accommodate up to 8 oxygen atoms, as in α-UO_3 and UO_2) to the coupling of two molecules of acetylene [19] (as well as ethylene [20]) to furan. We do not think that this is the case for furan formation from acetaldehyde. On the contrary, we think that furan is made from the aldol product that gives either furan or crotonaldehyde. The aldol is made through the condensation of two molecules of acetaldehyde as follows:

$$CH_3CHO + \mathbf{O}(s) \rightarrow {-}CH_2CHO(a) + \mathbf{O}H(a),$$

$$-CH_2CHO(a) + CH_3CHO(a) \rightarrow CH_3{-}\overset{\displaystyle O^-}{\overset{|}{C}}{-}CH_2{-}CHO(a),$$
(H)

$$CH_3{-}\overset{\displaystyle O^-}{\overset{|}{C}}{-}CH_2{-}CHO(a) + \mathbf{O}H(a)$$
(H)

$$\rightarrow CH_3{-}\overset{\displaystyle OH}{\overset{|}{C}}{-}CH_2{-}CHO(a) + \mathbf{O}(s),$$
(H)

$$CH_3{-}\overset{\displaystyle OH}{\overset{|}{C}}{-}CH_2{-}CHO(a) + \mathbf{O}(s) \rightarrow \text{(furan)} + 2H_2O,$$
(H)

$$CH_3{-}\overset{\displaystyle OH}{\overset{|}{C}}{-}CH_2{-}CHO(a) \rightarrow CH_3CH{=}CHCHO + H_2O,$$
(H)

$$CH_3CH{=}CHCHO + \mathbf{O}(s) \rightarrow \text{(furan)} + H_2O.$$

Crotonaldehyde is formed via dehydration of the aldol product, while furan formation requires cleavage of a C–H bond from the terminal CH_3 group of either the adsorbed aldol or the adsorbed crotonaldehyde. This requires strong oxidation sites (specific oxygen atoms) that are most likely present at low coverage only and that may explain the preferential formation of furan in this condition. If this is the case, then this process is activated, and once furan is formed it desorbs and that may explain its absence in the IR spectrum. At high initial surface coverage most of these sites are consumed for the condensation reactions and the reaction product is mainly crotonaldehyde.

5. Conclusions

The complex chemistry associated with the uranium oxides provides a rich example for studying the effect of bulk transformation on the surface reactions of simple oxides. In this work we have seen three types of reactions triggered by three different phases of the oxide. The simplest is the aldolization reaction of two molecules of acetaldehyde to crotonaldehyde on U_3O_8. This reaction is relatively common and other oxides (such as Al_2O_3 and TiO_2) show similar behavior. However, over β-UO_3, the condensation does not stop at crotonaldehyde formation, but a cyclization to furan occurs. The fact that the condensation, but not the cyclization, occurs on U_3O_8 is rationalized by the presence of specific oxygen sites on β-UO_3 that can abstract the H–C bond of terminal CH_3 of crotonaldehyde and result in reduction to UO_2 (on water elimination). Reduction reactions were observed mainly on UO_2 where both ethanol and C4 hydrocarbons were the dominant species. In situ IR data showed that acetaldehyde is adsorbed mainly parallel to the surface of UO_2, and this configuration is most likely a precursor to the coupling to a pinacolate intermediate in the process of making the C4 hydrocarbons by reductive coupling.

References

[1] B.E. Kahn, R.D. Rieke, Chem. Rev. 88 (1988) 733.
[2] Heinemann, J. Organomet. Chem. 201 (1995) 501.
[3] T.J. Marks, Prog. Inorg. Chem. 25 (1979) 224.
[4] D.C. Bradley, J.S. Ghotra, P.R. Raithket, Chem. Soc. Dalton Trans. (1977) 1166.

[5] M. Seth, M. Dolg, P. Fulde, P. Schwerdtfeger, J. Am. Chem. Soc. 117 (1995) 6597.
[6] M. Pepper, B.E. Bursten, Chem. Rev. 91 (1991) 719.
[7] K.S. Pitzer, Acc. Chem. Res. 12 (1979) 271.
[8] G.C. Allen, P.A. Tempest, J. Chem. Dalton Trans. (1982) 2169.
[9] G.C. Allen, N.R. Holmes, J. Appl. Spectrosc. 38 (1993) 124.
[10] C.A. Colmenares, Prog. Solid State Chem. 9 (1975) 139.
[11] F. Nozaki, K. Ohki, Bull. Chem. Soc. Jpn. 45 (1972) 3473.
[12] S. Sampath, K. Kulkarni, M.S. Subramanium, N.C. Jayadevan, Carbon 26 (1988) 129.
[13] F. Nozaki, F. Matsukawa, Y. Mano, Bull. Chem. Soc. Jpn. 48 (1975) 2764.
[14] G.J. Hutchings, C.S. Heneghan, I.D. Hudson, S.H. Taylor, Nature 384 (1996) 341.
[15] C.S. Heneghan, G.J. Hutchings, S.R. O'Leary, V.J. Boyd, S.H. Taylor, I.D. Hudson, Catal. Today 54 (1999) 3.
[16] R.K. Grasselli, J.D. Burrington, Adv. Catal. 30 (1981) 133.
[17] H.W.G. Heynes, C.G.M.C. Berkel, H.S. Van Der Ban, J. Catal. 48 (1977) 386.
[18] H. Madhavaram, P. Buchanan, H. Idriss, J. Vac. Sci. Technol. A 15 (1997) 1685.
[19] H. Madhavaram, H. Idriss, J. Catal. 206 (2002) 155.
[20] H. Madhavaram, H. Idriss, Stud. Surf. Sci. Catal. 110 (1997) 265.
[21] H. Madhavaram, H. Idriss, Catal. Today 63 (2000) 309.
[22] H. Madhavaram, H. Idriss, J. Catal. 184 (1999) 553.
[23] S.D. Senanayake, S.V. Chong, H. Idriss, Catal. Today 85 (2003) 311.
[24] F.Q. Yan, M.H. Qiao, X.M. Wei, Q.P. Lui, J. Chem. Phys. 111 (1999) 8068.
[25] K. Othmer, Encyclopedia of Chemical Technology, vol. 11, third ed., Wiley, New York, 1982.
[26] M.A. Henderson, Y. Zhou, J.M. White, J. Am. Chem. Soc. 111 (1989) 1185.
[27] W.S. Sim, P. Gardner, D.A. King, J. Am. Chem. Soc. 118 (1996) 9953.
[28] R.W. McCabe, C.L. DiMaggio, R.J. Madix, J. Phys. Chem. 89 (1985) 854.
[29] J.L. Davis, M.A. Barteau, J. Am. Chem. Soc. 111 (1989) 1782.
[30] C.J. Houtman, M.A. Barteau, J. Catal. 130 (1991) 528.
[31] L.-Q. Wang, K.F. Ferris, S. Azad, M.H. Engelhard, C.H.F. Peden, J. Phys. Chem., in press.
[32] H. Idriss, K.S. Kim, M.A. Barteau, J. Catal. 139 (1993) 119.
[33] M.A. Natal-Santiago, J.M. Hill, J.A. Dumesic, J. Mol. Catal. A 199 (1999) 140.
[34] W. Ji, Yi Chen, H.H. Kung, Appl. Catal. A 161 (1997) 93.
[35] S.C. Luo, J.L. Falconer, Catal. Lett. 57 (1999) 89.
[36] H. Idriss, C. Diagne, J.P. Hindermann, A. Kiennemann, M.A. Barteau, J. Catal. 155 (1995) 219.
[37] A. Yee, S. Morrison, H. Idriss, J. Catal. 186 (1999) 279.
[38] R.J. Madix, T. Yamada, S.W. Johnson, Appl. Surf. Sci. 19 (1984) 43.
[39] A. Beltramone, M. Gomez, L. Pierella, O. Anunziata, Molecules 5 (2000) 610.
[40] H. Hollenstein, H. Gunthard, Spectrochim. Acta A 27 (1971) 2027.
[41] J.M. Vohs, M.A. Barteau, Langmuir 5 (1989) 965.
[42] A. Yee, S.J. Morrison, H. Idriss, J. Catal. 191 (2000) 30.
[43] B.A. Sexton, Surf. Sci. 163 (1985) 99.
[44] R.M. Ormerod, C.J. Baddeley, C. Hardcare, R.M. Lambert, Surf. Sci. 360 (1996) 1.
[45] J.L. Davis, M.A. Barteau, Surf. Sci. 370 (1997) 113.
[46] K.T. Queeney, C.R. Arumainayagam, A. Balaji, C.M. Friend, Surf. Sci. 418 (1998) L31.
[47] K.T. Queeney, C.R. Arumainayagam, M.K. Weldon, C.M. Friend, M.Q. Blumberg, J. Am. Chem. Soc. 118 (1996) 388.
[48] R.J. McEachern, P. Taylor, J. Nucl. Mater. 254 (1998) 87, and references therein.
[49] Hj. Matzke, Radiat. Eff. 64 (1982) 3.
[50] X. Wang, Yi Fu, R. Xie, J. Nucl. Mater. 257 (1998) 287.
[51] L.H. Lu, K. Domen, K. Maruya, Y. Ishimura, I. Yamagami, T. Aoki, N. Nagato, Reac. Kinet. Catal. Lett. 64 (1998) 15.
[52] J.E. Rekoske, M.A. Barteau, Langmuir 15 (1999) 2061.
[53] R.P. Young, N.J. Sheppard, J. Catal. 7 (1967) 223.
[54] H.J. Oelichmann, D. Bougeard, B. Schrader, J. Mol. Struct. 77 (1981) 179.
[55] R.N. Spitz, J.E. Barton, M.A. Barteau, M.A. Staley, A.W. Sleight, J. Phys. Chem. 90 (1986) 4067.
[56] J. Boaventura, PhD thesis, University of Delaware, 1989.
[57] A.A. El-Azhary, R.H. Hilal, Spectrochim. Acta 53 (1997) 1365.